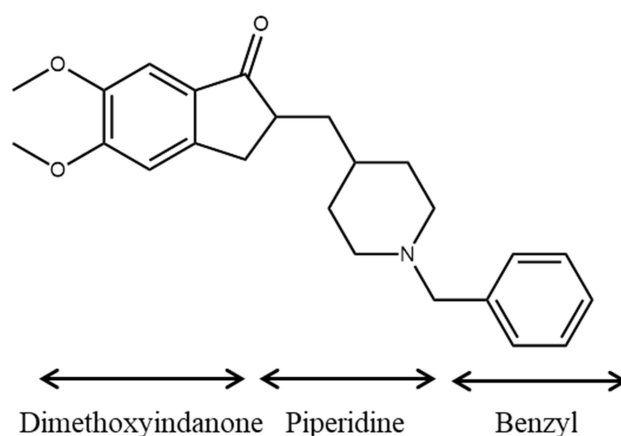


**Chapter 2**  
**(Review of Literature)**



## 2.1. Benzylpiperidine and benzylpiperazine derivatives as MTDL for AD

Donepezil is the most effective AChE inhibitor and most often prescribed medication for the treatment of AD. The N-benzylpiperidine nucleus is present in Donepezil as a core group. The structural framework of donepezil has been reported to suggest that a modification in this N-benzylpiperidine significantly lowers the AChE inhibitory activity (Figure 2.1) [Kryger et al. 1999]. Also, it was shown that N-benzylpiperidine ring of co-crystallized ligand i.e. donepezil (PDB: 4EY7) was extended into the CAS (Ser203, Glu334, and His447) while indenone moiety has shown significant binding towards PAS (Tyr72, Asp74, Tyr124, Trp286, and Tyr341), which are active pockets of hAChE [Caliandro et al. 2018]. In addition to these findings, N-benzylpiperidine ring has a basic nitrogen moiety that undergoes protonation at physiological pH, and leads to its increased affinity towards AChE and aspartate dyad (Asp32 and Asp 228) of BACE-1 (PDB: 2ZJM) along with significant BBB permeability due to acid-base equilibrium [Peauger et al. 2017]. All these findings have prompted several researchers to develop its congeners and, an extensive research effort has been made to explore and develop the N-benzylpiperidine and benzylpiperazine (bioisosteric form of benzylpiperidine) analogues as a MTDL for AD treatment.



**Figure 2.1.** Structural representation of Donepezil

Piemontese et al. have performed structure-based design approach for designing a series of some donepezil-like molecular hybrids. These derivatives were synthesized and biologically evaluated against AD treatment. Their work demonstrated that compounds **1** and **2** containing benzylpiperazine moiety had a better AChE inhibitory activity as compared to the piperidine analogs (Figure 2.2). They also found that the compound containing benzylpiperazine ring had A $\beta$  aggregation, antioxidant, and reduced A $\beta$ -induced cell toxicity [Piemontese et al. 2018].

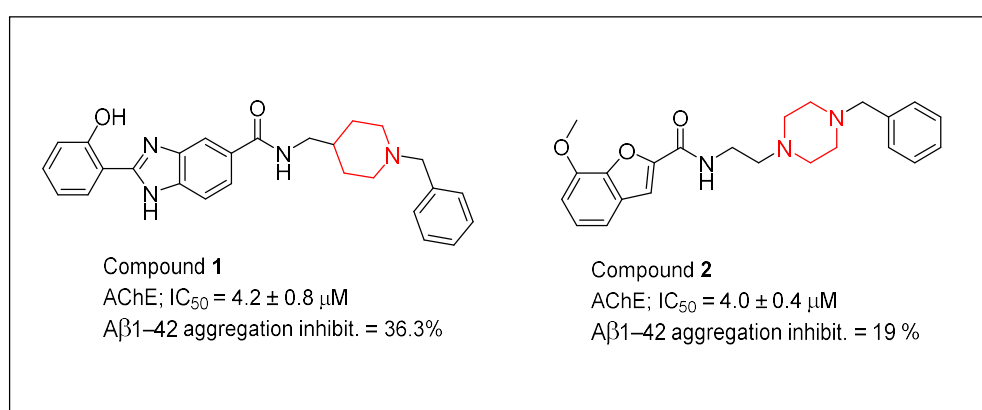


**Figure 2.2.** Structures of the benzylpiperidine and benzylpiperazine derivatives **1-2**

Hussein W et al. designed, synthesized and biologically evaluated some tacrine-based compounds having (thiocarbamoylthio) acetamide group linked with piperazines which may be responsible for enhanced ChE activity. The compound **3** containing 4-trifluoromethyl benzylpiperazine scaffold demonstrated good AChE and BChE inhibitory activity with good BBB permeability as compared to standard Tacrine and Donepezil (Figure 2.3) [Hussein et al. 2018].

Saeedi et al. explored the design, synthesized and biologically evaluated some aryl isoxazole-phenylpiperazines as potential ChEIs. Amongst them, compound **4** showed the highest inhibition of AChE and BACE-1 with neuroprotective activity (Figure 2.3). *In*

*silico* study suggested active site interactions with CAS and PAS residues of AChE by compound **4** [Saeedi et al. 2019].

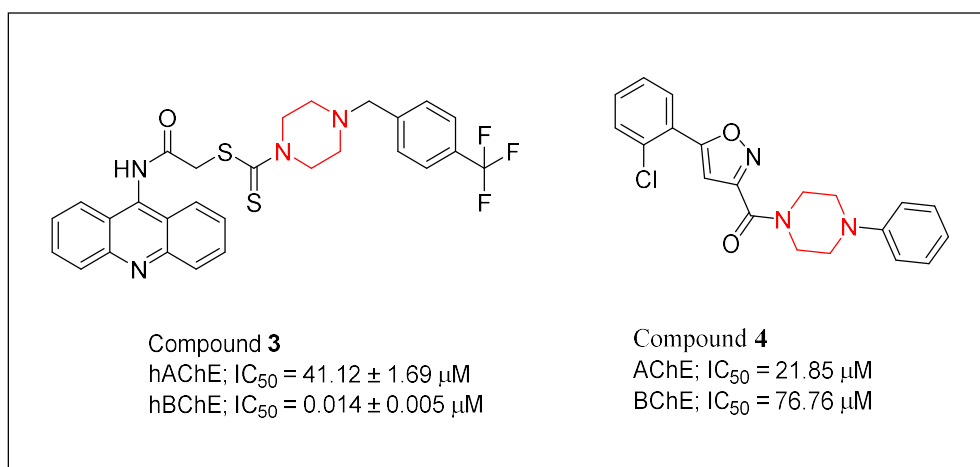


**Figure 2.3.** Structures of the benzylpiperidine and benzylpiperazine derivatives **3-4**

Du H. et al. designed and synthesized some deoxyvasicinone-benzylpiperazine fused derivatives as MTDL and biologically evaluated them against various targets for AD. Amongst them, compounds **5-8** exhibited hAChE, BACE-1, and Aβ aggregation inhibition potential. Additionally, compounds **5** and **7** also possess low cytotoxicity along with neuroprotective effects against SH-SY5Y cell lines (Figure 2.4) [Du et al. 2019].

Umar et al. have developed 1H-pyrazolo[3,4-b]pyridine derivatives as anti-AD. The most potential compounds **9** and **10**, demonstrated the selective anti-AChE, with little BChE inhibition property. Besides, Compound **11** showed Aβ aggregation (self and metal-induced) inhibition potential up to 81.65% along with disaggregation of 79.47%, antioxidant, and metal chelation properties (Figure 2.5) [Umar et al. 2019].

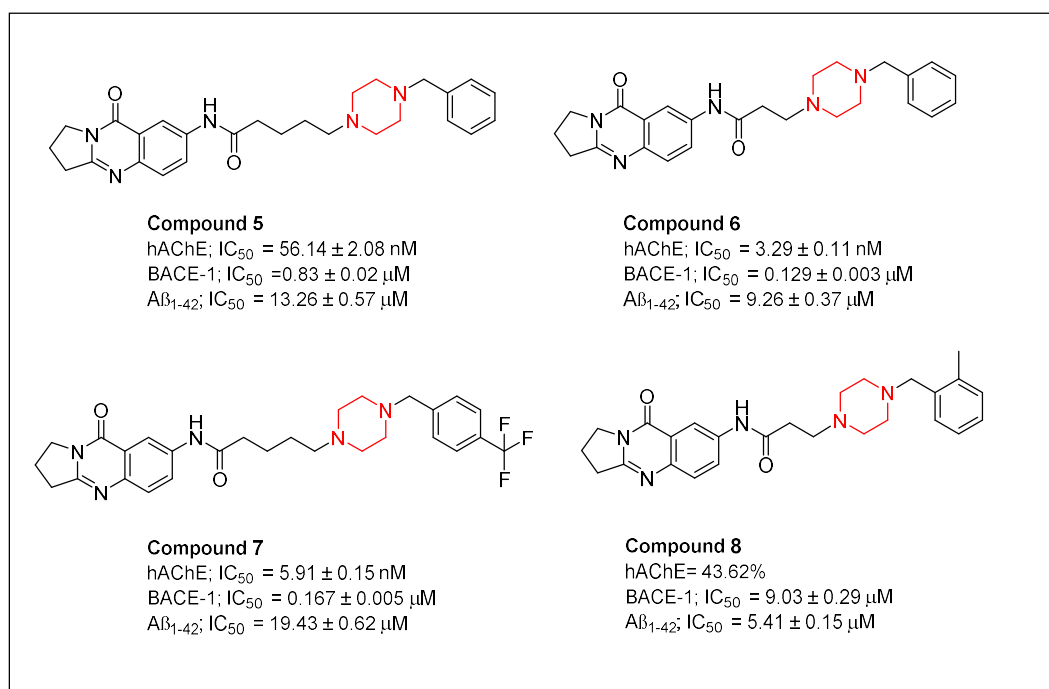


**Figure 2.4.** Structures of the benzylpiperidine and benzylpiperazine derivatives **5-8**

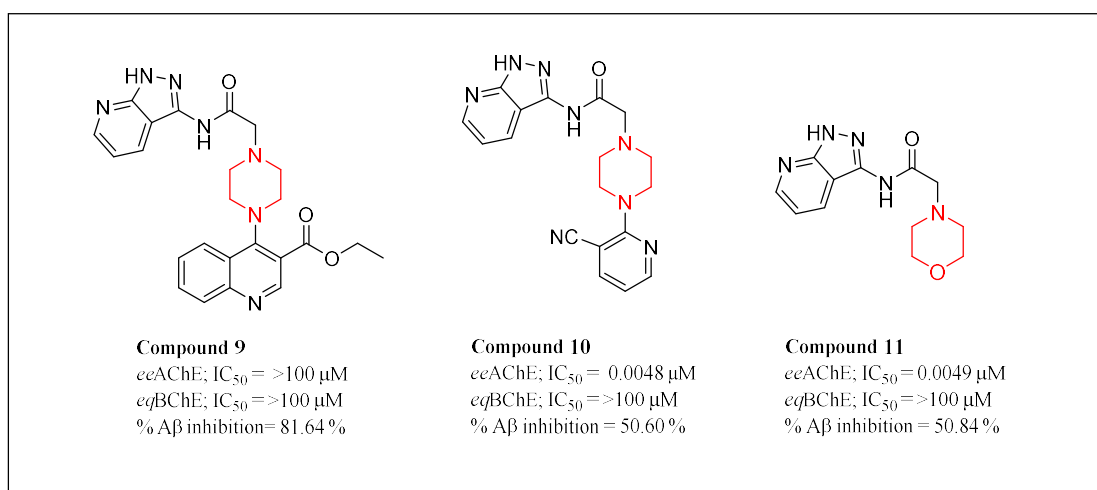


**Figure 2.5.** Structures of the benzylpiperidine and benzylpiperazine derivatives **9-11**

In a recent study, Greunen et al. designed novel *N*-benzylpiperidine carboxamide derivatives as potential ChE inhibitors for the treatment of AD. The two most active analogs of the series (compounds **12** and **13**, Figure 2.6) afforded *in-vitro* AChE inhibition with IC<sub>50</sub> values of 0.41 and 5.94 μM, respectively. *In silico* molecular docking and dynamics study showed similar binding patterns of these hybrids with donepezil against AChE [van Greunen et al. 2019].

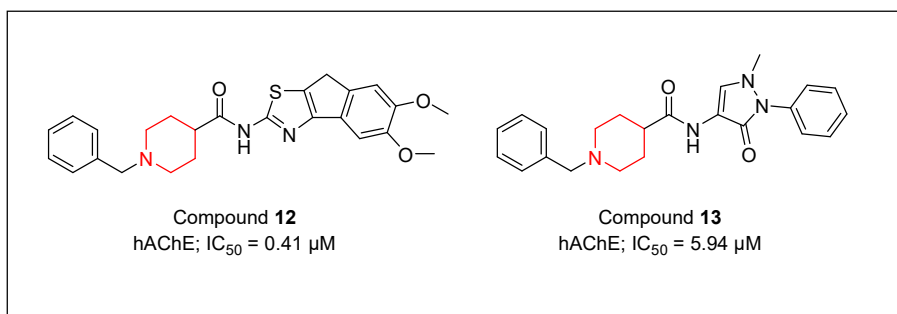


**Figure 2.6.** Structures of the benzylpiperidine and benzylpiperazine derivatives **12-13**

Sharma et al. in their work reported N-benzylpiperidine analogs as MTDL for the treatment of AD. Compound **14** (hAChE IC<sub>50</sub> = 0.072 μM; hBChE IC<sub>50</sub> = 7.8 μM; and hBACE-1 IC<sub>50</sub> = 0.43 μM) and **15** (hAChE IC<sub>50</sub> = 0.11 μM; hBChE IC<sub>50</sub> = 3.0 μM; and hBACE-1 IC<sub>50</sub> = 0.22 μM) among their designed compounds exhibited balanced multifunctional potential in micromolar to submicromolar range (Figure 2.7). Additionally, both compounds have also demonstrated anti-Aβ aggregation in self- and AChE-induced thioflavin T assay with excellent BBB permeability in PAPMA-BBB assay. Both compounds also demonstrated AChE-PAS binding in PI-displacement assay and the neuroprotective potential of the compound against SH-SY5Y cell lines. The *in-vivo* results of compound **32** demonstrated reversal of cognitive dysfunction in scopolamine and Aβ-induced animal models. While *ex-vivo* studies on brain homogenate demonstrated the anti-oxidant potential of the compounds [Sharma et al. 2019b].

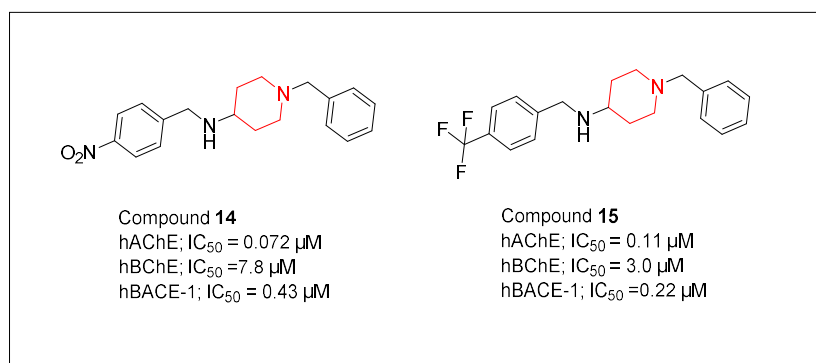


**Figure 2.7.** Structures of the benzylpiperidine and benzylpiperazine derivatives **14-15**

Chaves et al. reported the synthesis and *in-vitro* biological studies of hydroxy benzimidazole-donepezil (mimetic) hybrids as multitarget-directed ligands for AD treatment. Compounds **16** ( $IC_{50} = 1.8 \mu\text{M}$ ), **17** ( $IC_{50} = 1.8 \mu\text{M}$ ), and **35** ( $IC_{50} = 1.8 \mu\text{M}$ ) from their synthesized compounds demonstrated good AChE inhibitory activity in the micromolar range. Furthermore, compounds 87, 80, and 81 also exhibited anti-A $\beta$  aggregation potential in self and Cu (II) induced thioflavin T experiments, Additionally, compounds **16-18** have shown increased cell viability and neuroprotective activity against SH-SY5Y cell lines (Figure 2.8) [Chaves et al. 2020].

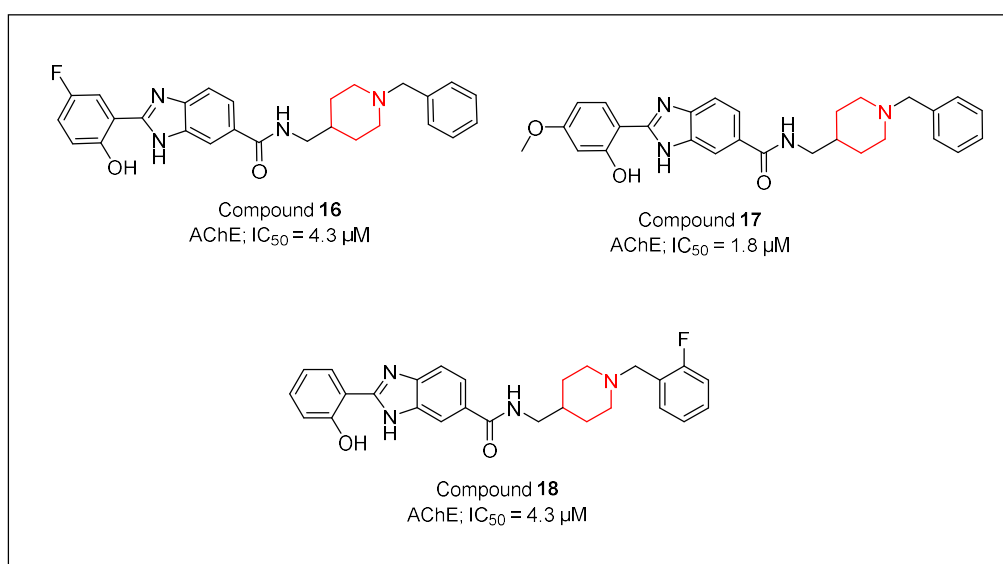


**Figure 2.8.** Structures of the benzylpiperidine and benzylpiperazine derivatives **16-18**

Makhaeva et al. reported amridine-piperazine hybrids as multifunctional agents for AD therapy. Their work demonstrates compound **19** (hAChE  $IC_{50} = 1.83 \mu\text{M}$  and hBChE  $IC_{50} = 10.1 \mu\text{M}$ ) as the most potent ChE inhibitory compound (Figure 2.9). Along with ChE inhibition, compound **19** also showed AChE-PAS binding in PI-displacement assay, antioxidant activity, and radical scavenging activity additionally demonstrated multifunctional property of the compound [Makhaeva et al. 2021].

Karaca et al. have reported novel benzothiazole liked piperazine derivatives as MTDL for AD treatment. The most active compound from their series **20** exhibited good ChE (AChE  $IC_{50}$  = 23.4 nM and BChE  $IC_{50}$  = 32.8 nM) and MAO (MAO-A  $IC_{50}$  = 41.3 nM and MAO-B  $IC_{50}$  = 40.3 nM) dual inhibitory activity (Figure 2.9). Additionally compound **20** also exhibited anti-A $\beta$  aggregation and non-neurotoxic profile of the compound suggesting overall multifunctional inhibitory property of the compound against AD [Karaca et al. 2022].

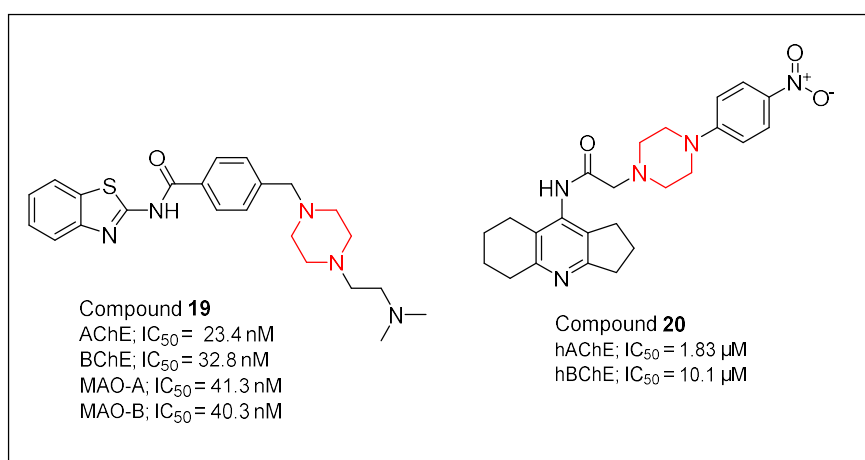


**Figure 2.9.** Structures of the benzylpiperidine and benzylpiperazine derivatives **19-20**

Qin et al. have demonstrated N-benzylpiperidine derivatives as multifunctional inhibitors. Compound **21** (HDAC  $IC_{50}$  = 0.17  $\mu$ M, AChE  $IC_{50}$  = 6.89  $\mu$ M), and **22** (HDAC  $IC_{50}$  = 0.17  $\mu$ M, AChE  $IC_{50}$  = 6.89  $\mu$ M), among their tested derivatives, exhibited multifunctional inhibitory activity including free radical scavenging, metal chelation and anti-A $\beta$  activity (Figure 2.10). Both compounds also demonstrated neuroprotective and AChE selectivity profile suggesting MTDL ability of the compounds [Qin et al. 2023].

Jaipea et al. recently reported piperine analogs as dual ChE inhibitors. Compound **23** was the most potent ChE inhibitor. The pharmacokinetic study of the compound **23** against AChE also revealed competitive inhibition while it showed noncompetitive inhibition

against BChE enzymes (Figure 2.10). The inhibition constant ( $K_i$ ) value of the compound also demonstrated its binding with ChE enzymes [Jaiepa et al. 2023].

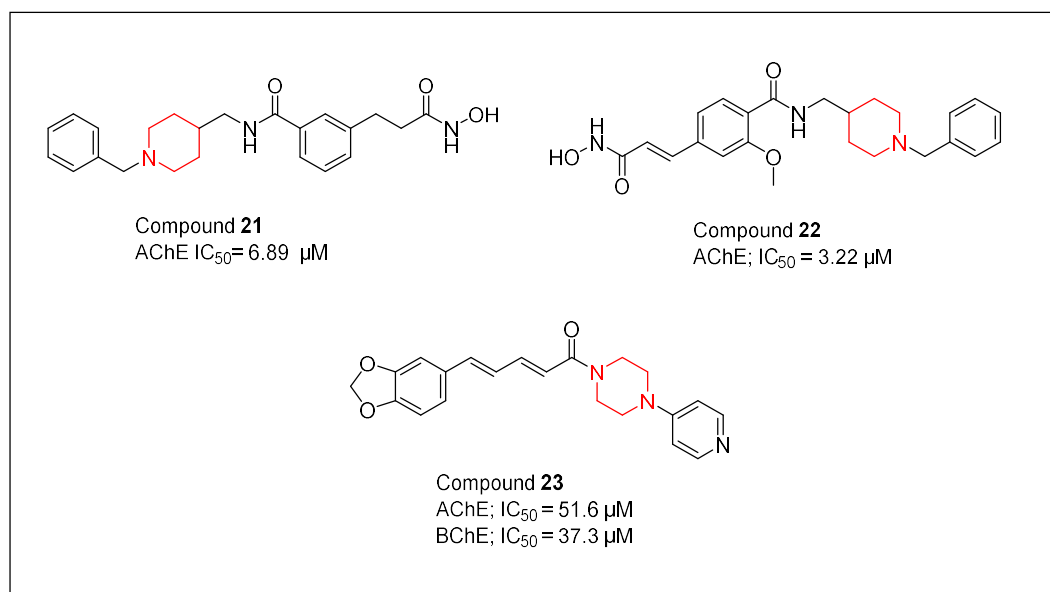


**Figure 2.10.** Structures of the benzylpiperidine and benzylpiperazine derivatives **21-23**

## 2.2. Quinazoline derivatives

Gokhan-Kelekçi et al. designed a novel series of pyrazoline derivatives incorporating quinazolinone scaffold and evaluated their MAO-A and MAO-B inhibitory activities. In their work it was found that compound **24** (2-((Z)-2-((E)-3-(5-chlorocyclohexa-1,3-dien-1-yl)-1-phenylallylidene)hydrazinyl)-3-methylquinazolin-4(3H)-one) (Figure 2.11) was a potential candidate against both the enzymes. Over-activation of MAO-B is responsible for a neurodegenerative disorder like AD. To understand the interaction involved between the MAO active site and the designed molecule, molecular docking studies were performed. Compound **24** was able to selectively inhibit MAO-B as compared to MAO-A. The docking results of compound **24** have shown hydrophobic linkage and  $\pi$ - $\pi$  stacked interaction with F343 and Y398 respectively with MAO-B. The inhibitory activity of compound **24** was compared with porgyline (standard MAO-B inhibitor), and their findings suggested that compound **24** (MAO-B;  $IC_{50}$  =  $1.15 \pm 0.12$   $\mu$ M) was better than

the standard compound porgyline (MAO-B;  $IC_{50} = 3.35 \pm 0.23 \mu\text{M}$ ). From SAR studies, the addition of chlorine on the phenyl ring of the derivatives was responsible for the MAO-inhibitory activity. Amongst them, compound **24** having chlorine at meta-position of the phenyl ring tended to inhibit MAO-B effectively while derivatives having chlorine at the para-position inhibit MAO-A. Thus, finding based on biological evaluations and interaction properties with the receptor suggested that quinazoline-based analogs can further be utilized as a lead in the development of anti-Alzheimer agents [Gökhan-Kelekçi et al. 2009].

Varadi et al. synthesized and provided a configurational evaluation of designed 1-substituted derivatives of imidazoquinazolidione by thermal cyclo-condensation of 4-oxo-quinazoline-2-carboxamide with a series of aldehydes and ortho esters. The separation and elucidation of the enantiomers were taken place with the help of chiral HPLC and CD. It was found that the compounds were highly potent antagonists with nanomolar affinity in the [ $^3\text{H}$ ] 5, 7 dichlorokynurenic acid binding assay and interacted with glycine residue of NMDA receptors. Among them, compound **25** (N-(4-(3,9-dioxo-1,2,3,9-tetrahydroimidazo[5,1-b]quinazolin-1-yl)phenyl)acetamide) (Figure 2.11) was proved to be the most active compound having  $K_i = 8 \text{ nM}$ . The absolute configuration of specific enantiomers was further evaluated with the help of HPLC-ECD spectra. Based on the above analysis, the introduction of N-phenylacetamide at 1 position of imidazoquinazolidiones might be useful as a lead compound in the management of AD [Váradi et al. 2012].

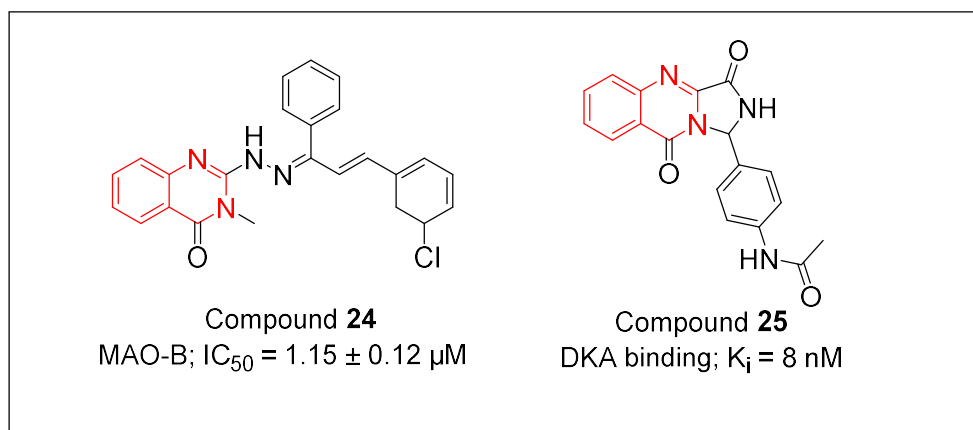


**Figure 2.11.** Structures of the quinazoline derivatives **24-25**

Yu C-W et al. designed and synthesized quinazoline-4-one derivatives bearing a hydroxamic acid scaffold. All the reported compounds were evaluated for HDAC enzymatic inhibition assay and it was found that all the compounds were highly potent HDAC inhibitors. Amongst them, compound **26** ((E)-3-(2-Ethyl-7-fluoro-4-oxo-3-phenethyl-3,4-dihydroquinazolin-6-yl)N-hydroxyacrylamide), was the most promising HDAC-6 inhibitor ( $IC_{50} = 8 \text{ nM}$ ) (Figure 2.12). Another compound **27** (N-Hydroxy-3-(2-methyl-4-oxo-3-phenethyl-3,4-dihydro-quinazolin-7-yl)-acrylamide), has gained a tendency to selectively binds and inhibit the HDAC-6 ( $IC_{50} = 29 \text{ nM}$ ). Trichostatin A, a PAN HDAC inhibitor was taken as a standard compound but it did not show expected results and selectivity profile. Compounds **26** and **27** were further analyzed by neurite outgrowth assay and it was found that they showed induced substantial neurite outgrowth on PC12 and SH-SY5Y cells lines at  $10 \mu\text{M}$  concentration. The expression of  $\alpha$ -Actubulin and Ac-histone levels in PC12 neurons were analyzed by introducing compounds **26** and **27** and they found that compound **27** (Figure 2.12) enhanced the level of  $\alpha$ -Actubulin and Ac-histone H3 appropriately at  $10 \mu\text{M}$  concentration. The effects of the inhibitors on learning-impaired mice with hippocampal lesions (generated by zinc-mediated  $A\beta$  aggregates) were tested using the accelerated Rota-rod test. When compared to control, the learning-based performances of the mice injected with compounds **26** or **27**

improved with time. Furthermore, it was discovered that compounds **26** and **27** had elevated the Ac-tubulin level inside the hippocampal region of lesion mice. The suppression of HDAC-6 in the brain of mice was found to be responsible for the learning-based performance enhancement. The SAR studies suggested that the application of alkyl substituted phenyl linker groups rather than phenyl alone at position 3 produced significant results and forced the entry of the compound to the active target site and may act as a promising lead candidate in AD therapy [Yu et al. 2013].

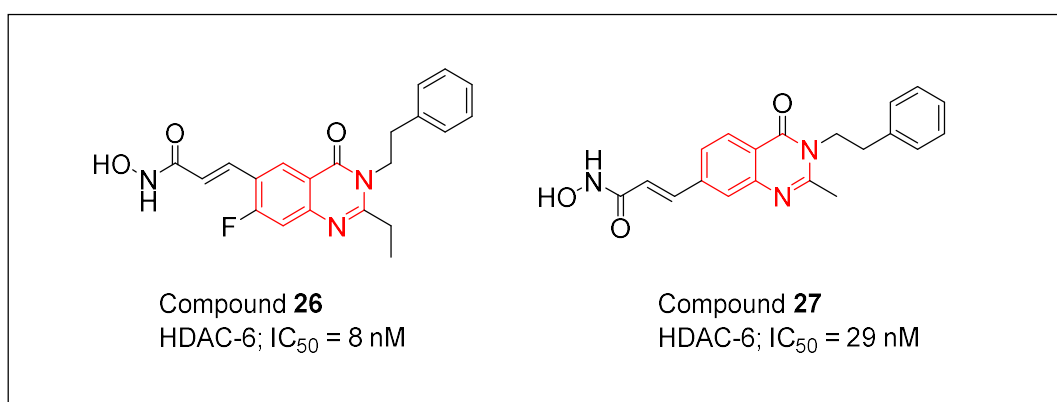


**Figure 2.12.** Structures of the quinazoline derivatives **26-27**

Iqbal J et al. reported a series of azomethine-dihydro-quinazolinone derivatives and evaluated them against the ChE enzymes. Most of the reported compounds from their work have shown promising results. The most active compound **28** ((E)-N'-(4-bromobenzylidene)-2-((4-oxo-3-(otolyl)-3,4-dihydroquinazolin-2-yl)thio)acetohydrazide) (Figure 2.13), from the designed conjugates, have shown IC<sub>50</sub> = 209.8 ± 1.11 μM against AChE and the results were compared to reference compound neostigmine having IC<sub>50</sub> = 24.3 ± 4.11 μM. The molecular docking studies were carried out and suggested that compound **28** was involved in forming two hydrogen bond interactions with Try124 and Arg296 amino acid residues of the AChE enzyme. Compound **28** was further analyzed for their binding energy profile and has shown (ΔG = - 12.89 kcal/mol) good stability amongst the synthesized compounds. From SAR studies, it was proved that the bromine

substitution at the 4<sup>th</sup> position in their synthesized derivative was responsible for AChE inhibitory activity. Hence, 4-bromo substituted azomethine-dihydro-quinazolinone conjugates can further be utilized as a lead compound for drug development to reduce the progression of AD [Iqbal et al. 2016].

Mohamed T et al. synthesized and evaluated 2, 4-disubstituted quinazoline derivatives as multi-functional agents in AD therapy. The biological assay revealed that most of their synthesized compounds had shown promising inhibitory potential against both the ChE enzymes. Amongst them, compound **29** (Figure 2.13) (N2-(1-benzylpiperidin-4-yl)-N4-(3,4-dimethoxybenzyl) quinazoline-2, 4-diamine) have shown ChE inhibitory activity (AChE; IC<sub>50</sub> = 2.1 μM, BuChE; IC<sub>50</sub> = 8.3 μM) and was comparable to standard compound donepezil (AChE; IC<sub>50</sub> = 0.03 μM, BuChE; IC<sub>50</sub> = 3.6 μM). Compound **29** was also capable of reducing Aβ aggregation (Aβ40: IC<sub>50</sub> = 2.3 μM) significantly. Compound **30** (4-(benzylamino) quinazoline-2-ol) was also considered as the excellent Aβ aggregation inhibitor (Aβ40; IC<sub>50</sub> = 0.27 μM) and was found to be four times more effective as compared to the standard compound curcumin (Aβ40; IC<sub>50</sub> = 3.3 μM). Further, the anti-oxidant property of compound **30** (Figure 2.13) was evaluated through DPPH radical scavenging assay and has shown 47% DPPH scavenging at 50 μM while resveratrol has shown 41.9%. The molecular docking studies suggested that N-2-1-benzylpiperidine of compound **29** was involved in hydrogen bond interaction as well as π-π stacking with Try341 of the PAS region. The quinazoline moiety of compound **30** was able to interact with the loop region consisting of Asn27- Gly29. From SAR studies, it was concluded that the 2 and 4 position of the quinazoline ring is important to design multi-targeting agents in the treatment of AD [Mohamed and Rao 2017].

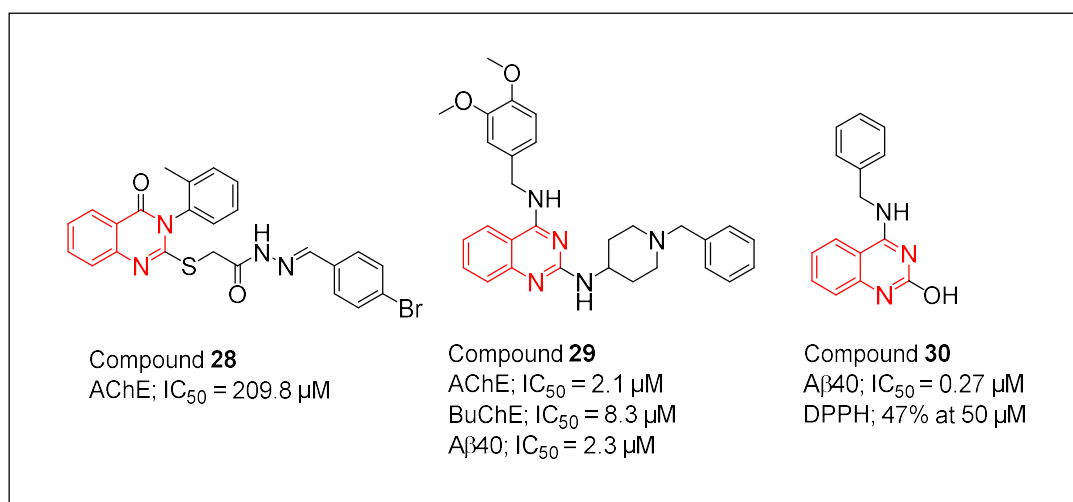


**Figure 2.13.** Structures of the quinazolinone derivatives **28-30**

Haghighijoo Z et al. designed, synthesized, and biologically evaluated quinazolinone-hydrazone derivatives as novel multi-targeting candidates essentially with improved BACE-1 inhibitory properties, improved BBB permeability, and desirable anti-oxidant characteristics for AD therapy. Amongst them, compound **31** ((E)-2-(2-(2,3-dichlorobenzylidene)hydrazinyl)-3-methylquinazolin-4(3H)-one) (Figure 2.14) containing 2, 3-dichlorophenyl group provided excellent inhibitory activity IC<sub>50</sub> = 3.7 μM against BACE-1. Similarly, compound **32** ((E)-2-(2-(2,4-dihydroxybenzylidene)hydrazinyl)-3-methylquinazolin-4(3H)-one) (Figure 2.14) containing 2, 4-dihydroxyphenyl moiety has shown optimum BACE-1 inhibitory potential (IC<sub>50</sub> = 27.6 μM) with a significant anti-oxidant effect (IC<sub>50</sub> = 8.4 μM). OM99-2 (Glu-Val-Asn-Leu-Ala-Ala-Glu-Phe) (IC<sub>50</sub> = 0.014 μM) and quercetin (IC<sub>50</sub> = 9.0 μM) were utilized as a standard BACE-1 inhibitor and DPPH radical scavenging compound, respectively. Based on docking studies of compound **31**, it was suggested that the carbonyl group of quinazolinone moiety was interacting with amino acid residues Asp228 as well as of Asp 32 via hydrogen bond interaction. SAR studies revealed that replacement of the chloro substituent from the 4- to 3-position generated 2, 3-dichloro substituted **31** acquiring excellent BACE-1 inhibitory potency. Based on the above facts, it was suggested that quinazolinone-hydrazone

derivatives may play an important role in the drug development for AD treatment [Haghighijoo et al. 2017].

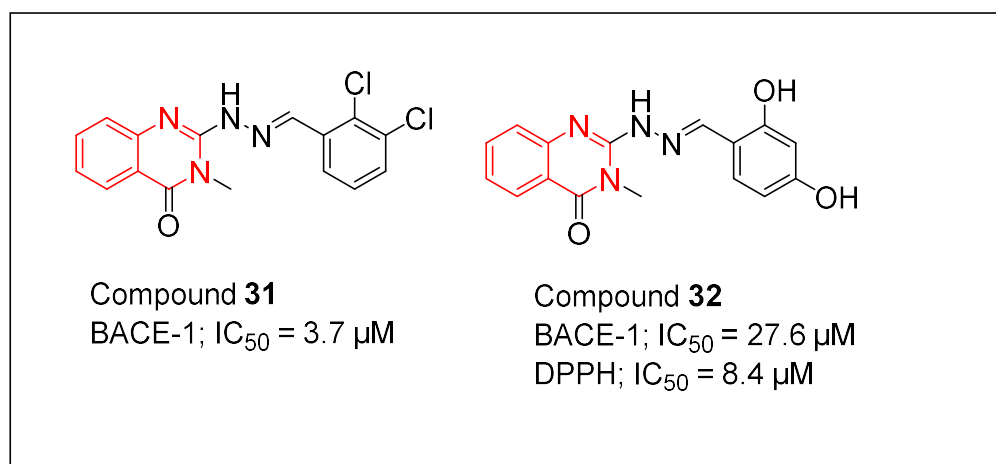


**Figure 2.14.** Structures of the quinazoline derivatives **31-32**

Ma F et al. developed a deoxyvasicinone derivatives having aminoacetamide group at 6 positions to obtain novel multi-targeting, anti-AD agents. *In-vitro* analysis revealed that most of the synthesized compounds acquired good inhibitory potency against both the ChE enzymes in a nanomolar range. Compound **33** (2-((3,5-difluorobenzyl)amino)-N-(9-oxo-1,2,3,9-tetrahydropyrrolo[2,1-b]quinazolin-7-yl)acetamide) (Figure 2.15) showed excellent inhibitory potential for AChE, with IC<sub>50</sub> = 7.61 ± 0.53 nM. It also acquired the better capability to inhibit BuChE, with IC<sub>50</sub> = 2.35 ± 0.14 nM than positive control tacrine (IC<sub>50</sub> = 10.8 nM) and demonstrated the promising inhibitory activity for Aβ<sub>(1-42)</sub> self-aggregation (63.9 ± 4.9%, 10 μM) with improved metal chelator properties. From the SAR studies, it was found that the introduction of saturated alkyl or aromatic moieties in the aminoacetamide group produced similar trends in both enzymes [Ma and Du 2017].

Sarfraz M et al. designed, synthesized, and evaluated several 2, 3- dihydro-quinazoline-4(1H)-one derivatives. The biological evaluation of the synthesized compounds suggested that most of the compounds were active against both ChE enzymes in the micromolar

range. Amongst them, compound **34** (6,8-dibromo-2-(4-chlorophenyl)-2-methyl-2,3-dihydroquinazolin-4(1H)-one) (Figure 2.15) can be regarded as a potential lead candidate with dual ChE inhibition potency with  $IC_{50} = 1.6 \pm 0.10 \mu\text{M}$  (AChE) and  $3.7 \pm 0.18 \mu\text{M}$  (BuChE) as compared to the reference drug galantamine with an  $IC_{50} = 4.0 \pm 0.10 \mu\text{M}$  (AChE) and  $15.0 \pm 0.67 \mu\text{M}$  (BuChE), respectively. SAR studies revealed that the application of the 4-chlorophenyl group at the C-2 position provides improved effects. Further, molecular docking analysis provided that di-bromo phenyl ring formed  $\pi$ - $\pi$  stacking with Trp86 in AChE, chlorophenyl moiety at C-2 position was also engaged in  $\pi$ - $\pi$  stacking with Tyr334 and Tyr337. Based on the above facts, it was proved that C-2 substituted 2, 3-dihydroquinazolin-4(1H)-one derivative may be a useful lead candidate in the treatment of AD [Sarfranz et al. 2017].

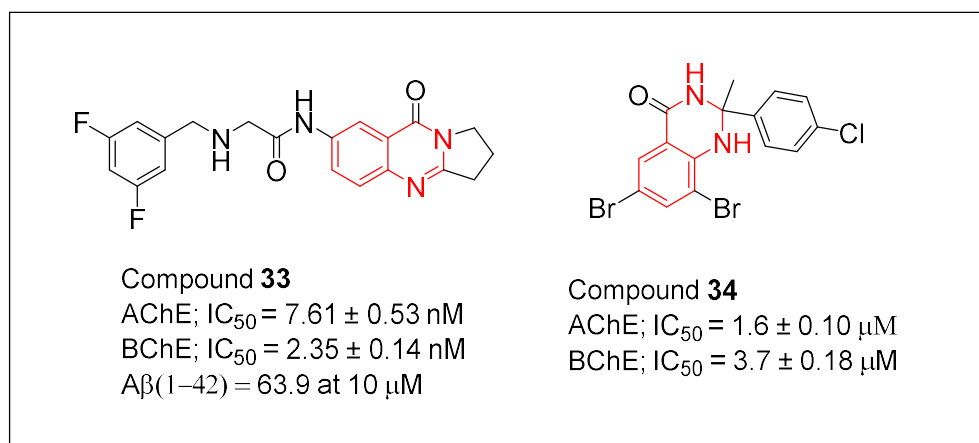


**Figure 2.15.** Structures of the quinazoline derivatives **33-34**

Mohamed T et al. designed, synthesized, and biologically evaluated the quinazoline and pyrido [3, 2-d] pyrimidine-based compounds as multi-functional candidates in the treatment of AD. Compound **35** (8-chloro-N2-isopropyl-N4-phenethylquinazoline-2, 4-diamine) (Figure 2.16) was found to be the most potent multi-functional agent amongst their series with  $A\beta_{40}$  aggregation inhibitory potential ( $IC_{50} = 900 \text{ nM}$ ) and was three times more effective as compared to the standard compound curcumin ( $A\beta_{40}$ ;  $IC_{50} = 3.3$

$\mu\text{M}$ ). It also acquired a dual AChE/BuChE inhibitory profile (AChE;  $\text{IC}_{50} = 8.6 \mu\text{M}$ , BuChE;  $\text{IC}_{50} = 2.6 \mu\text{M}$ ) while the reference compound donepezil showed an  $\text{IC}_{50} = 0.03 \mu\text{M}$  (AChE) and  $\text{IC}_{50} = 3.6 \mu\text{M}$  (BuChE) against both the ChE enzymes. SAR studies suggested that the introduction of chlorine at the C-8 position and isopropyl at the R1 position provides excellent results against A $\beta$ 40. Molecular docking studies conveyed that 8 chloro quinazoline was stacked parallel with Trp86 amino acid residue of PAS region and also could orient itself between C and N terminal region of A $\beta$  dimer while C-4 substituted phenethylamine derivative hydrophobically interacted with Asp23-Gly29 turn region. Based on the above investigations, it was stated that C-8 substituted quinazoline derivatives with isopropyl moiety would be considered as a promising lead compound in AD therapy [Mohamed et al. 2017].

Jagtap et. al. design, and synthesis of a series of 4-substituted 2-amino-3,4-dihydroquinazolines as novel inhibitors of BACE-1. Among these derivatives, compound **36** having 4-methyl-substituted 2-amino-3,4-dihydroquinazoline bearing a side chain of N-cyclohexyl-N-((1-methyl-1Hpyrazol-4-yl)methyl amide (Figure 2.16) exhibited potent BACE-1 inhibitory activity ( BACE-1 CFA  $\text{IC}_{50} = 0.38 \mu\text{M}$ ; BACE-1 WCA  $\text{IC}_{50} = 0.14 \mu\text{M}$ ) [Jagtap et al. 2020].

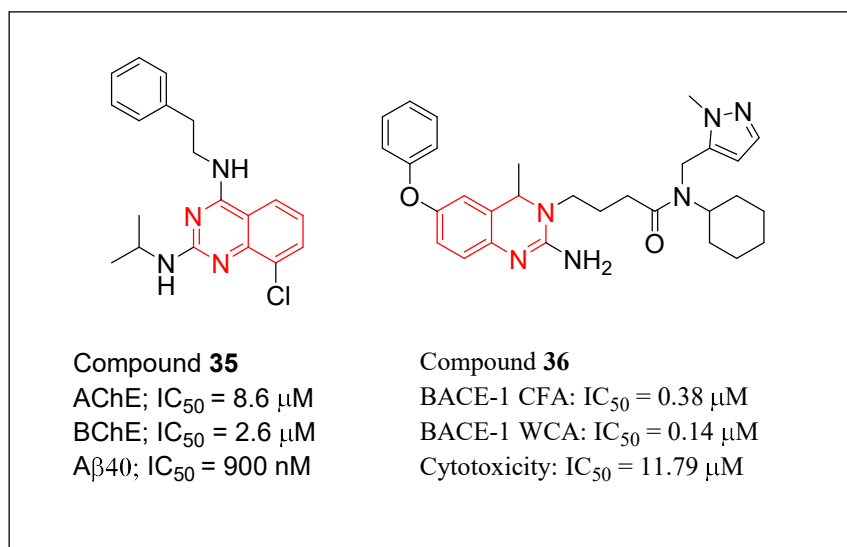


**Figure 2.16.** Structures of the quinazoline derivatives **35-36**

Li Zeng et al. designed and synthesized a series of novel 2-(2-indolyl)-4(3H)-quinazolines derivatives based on SBDD approach and by removal of the methylene groups in 7, 8 positions of the rutaecarpine C-ring alkaloid and introduction of side chain with terminal amino groups at the 3 or 5 position and biologically evaluated as AChE inhibitors. Among them, compound **37** having optimum chain length ( $n = 2$ ) and piperidine terminal moiety exhibited strong inhibitory activity for AChE and high selectivity for AChE over BuChE (AChE;  $IC_{50} = 20.97 \text{ nM}$ , BuChE;  $IC_{50} = 7.3 \mu M$ ) (Figure 2.17). The molecular docking studies also corroborated the *in-vitro* AChE findings suggesting good binding profile against hAChE enzyme [Li et al. 2013].

Svobodova B et al. designed, synthesized, and biologically evaluated 24 novel *N*-methylpropargylamino-quinazoline derivatives against various targets responsible for the AD. Amongst them, compound **38** was considered as the best candidate exhibited a selective MAO-B inhibition profile, NMDAR antagonism, an acceptable cytotoxicity profile, and the potential to permeate through BBB (Figure 2.17). Overall, compound **15** can be acts as a lead candidate for AD therapy [Svobodova et al. 2023].

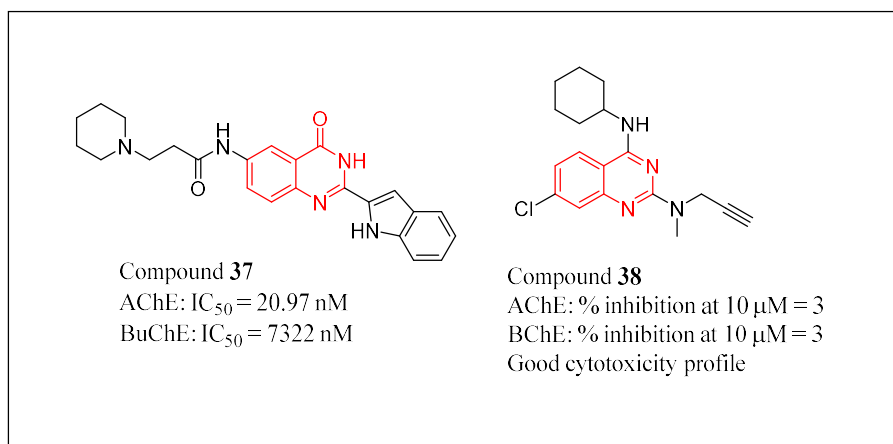


**Figure 2.17.** Structures of the quinazoline derivatives **37-38**

Wang B et al. designed and synthesized 3-aminoalkanamido-substituted rutaecarpine and 7,8-dehydro-rutaecarpine quinazolinones derivatives and subjected to biological evaluation. The results showed that the synthetic compounds possessed high AChE inhibitory potency. Compound **39** was the most potent for AChE inhibition, which presented an IC<sub>50</sub> value of 10.07 nM (Figure 2.18). The SAR suggested that the introduction of the aminoalkanamido-substituted group side chains could significantly increase the inhibitory activity of derivatives due to its protonation at physiological pH, thus occupying the anionic binding site of quaternary amino group via cation- $\pi$  interaction, and improved binding against PAS of AChE. The molecular docking, reversibility and kinetic analysis suggested that the compound **39** has shown good and reversible interactions towards active pocket of TcAChE. Overall, compound **39** represent useful candidate for the development of new anti-AD agents [Wang et al. 2010].

Zang L et al. designed and synthesized 1,2,3,9-tetrahydropyrrolo[2,1-b]quinazoline-1-carboxylic acid derivatives and their neuroprotective activity was estimated against NMDA-induced cytotoxicity *in-vitro*. Among these compounds, the compound **40** (78.6% at 100 μM) exhibited slightly higher potency than ifenprodil (65.1% at 100 μM) at the test concentration. In addition, the Ca<sup>2+</sup> influx induced by NMDA could be attenuated

significantly upon treatment with compound **40** via suppressing the NR2B up-regulation and increase p-ERK1/2 expression (Figure 2.18). Additionally, the docking results suggested that compound **40** might fit well with specific key interactions in the binding pocket of NR2B-selective NMDAR. According to the experiments results in this study, compound **40** made it a promising lead for the development of new potent and orally bioavailable NR2B-selective NMDAR antagonists [Zhang et al. 2018].

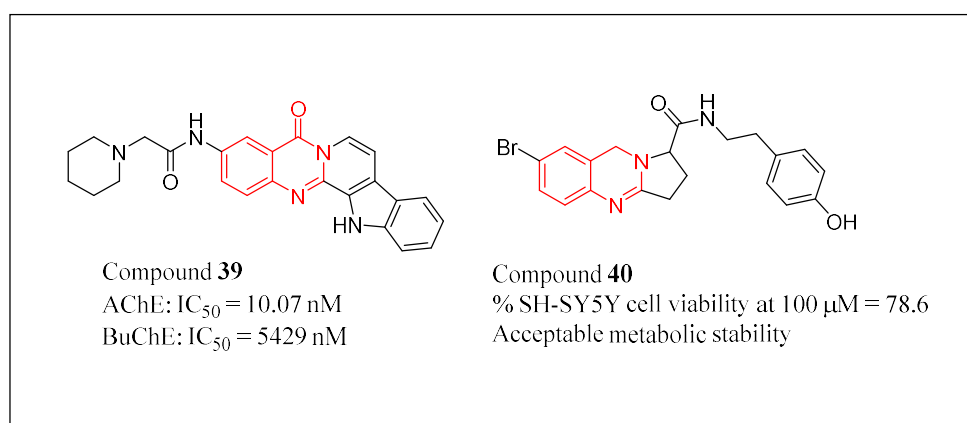


**Figure 2.18.** Structures of the quinazoline derivatives **39-40**

In the field of natural AChEIs, the methanol extracts of the seeds of genus *Peganum* exhibited significant inhibitory activity against this AChE and BuChE enzymes. By the isolation from *P. nigellastrum* Bunge, some alkaloids namely **deoxyvasicine**, **vasicine**, **vasicinone**, **deoxyvasicinone** were identified as potential natural AChE inhibitors. The **deoxyvasicine** and **vasicine** were the most potent BuChE inhibitors, displaying dual AChE/BuChE inhibitory profile (Figure 2.19) [Ma and Du 2017].

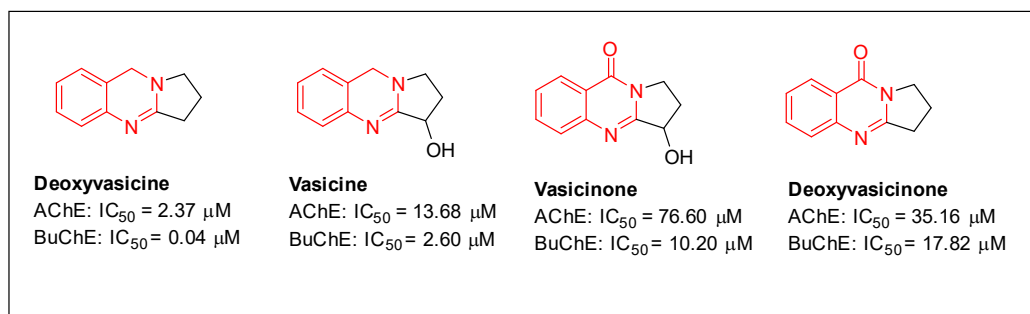


**Figure 2.19.** Structures of the quinazoline scaffold containing natural derivatives

### 2.3. Drugs under clinical investigations for AD

There are several potential drug candidates under various clinical phase trials and are continuously being evaluated to develop promising agents with anti-AD effects to cure and mitigate AD. We have summarized some of the recent drugs and vaccines which are either FDA approved or under clinical development and categorized them under the following phases (Figure 2.20) (Table 2.1).

Phase I	Phase II	Phase III	FDA approved drugs
<ul style="list-style-type: none"> <li>• AD-01</li> <li>• AD-02</li> <li>• CTI1812</li> <li>• TPI-287</li> </ul>	<ul style="list-style-type: none"> <li>• UB-311</li> <li>• ABT-288</li> <li>• GSK239512</li> <li>• Rilozole</li> <li>• Verubecestat</li> <li>• EVP-0962</li> <li>• Isopronidine</li> <li>• Epigallocatechin-3-gallate</li> <li>• NP-031112</li> </ul>	<ul style="list-style-type: none"> <li>• Encenidine</li> <li>• Bapineuzumab</li> <li>• Crenezumab</li> <li>• Aducanumab</li> <li>• TRx0237</li> <li>• Flurizan</li> <li>• Nilvadipine</li> <li>• Idalopirdine</li> <li>• Azeliragon</li> </ul>	<ul style="list-style-type: none"> <li>• Donepezil</li> <li>• Rivastigmine</li> <li>• Galantamine</li> <li>• Memantine</li> </ul>

**Figure 2.20.** Drugs under clinical investigation and FDA approved in AD therapy

### **2.3.1. Phase I**

Affitopes, short peptides of A $\beta$ <sub>(1-42)</sub> exhibited an ability to mimic in the same manner as that of A $\beta$ <sub>(1-42)</sub> but it does not have an identical sequence. There are several peptide affitopes are present but AD-01 and AD-02 (NCT01225809, NCT02008513) are mainly responsible for targeting the N-terminal A $\beta$  fragment. The results reveal that both are considered to be safe and significantly tolerated. To develop it as an anti-Alzheimer agent, dose optimization process is under evaluation [Reitz 2012]. TPI 287 (Figure 2.21) is a synthetic analog of taxane di-terpenoid tubulin acting and microtubule-stabilizing agent which is in Phase I clinical trial for mild to moderate AD patients. TPI 287 is responsible for stabilizing the mis-folding of tau protein in the brain (Clinical Trial Identifier: NCT01966666) [Hung and Fu 2017]. CT1812 (Figure 2.21) drug is recruiting phase 1b trails to study the possible effects on A $\beta$  oligomer displacement with mild to moderate AD patients after binding with sigma-2 receptor as an allosteric antagonist (NCT03522129) [Grundman et al. 2019].

### **2.3.2. Phase II**

UB-311 is a vaccine possessing an active immunotherapeutic strategy in which immunogen A $\beta$ <sub>(1-14)</sub> is linked with UBITH peptide (United Neuroscience Ltd.) and reported in suppression of production of severe anti-A $\beta$  immune activity. This study was performed in mild to moderate AD patients NCT03531710 (Figure 2.21) [Wang et al. 2017]. ABT-288 is a selective competitive H3 inhibitor for the treatment of cognitive deficits in AD and schizophrenia. The result indicated that Phase II trial of ABT-288 in mild-to-moderate AD patients as an adjoining therapy with donepezil was ended due to clinical inefficacy (Clinical Trial Identifier: NCT01018875) (Figure 2.21) [Haig et al. 2014]. In the same way, GSK239512 (Figure 2.21), a novel competitive inhibitor of H3

receptor was interrupted in Phase II clinical study due to inadequate memory impairment in mild-to-moderate AD patients (C.T.I.: NCT01009255). These findings revealed that H3 receptor antagonists are not a choice of an effective treatment in the cognitive dysfunction in AD [A Grove et al. 2014]. Riluzole (Figure 2.21) is a 2-amino-6-(trifluoromethoxy)benzothiazole derivative that helps in minimizing the TauP301L-mediated reductions in PSD-95 expression which is considered as a biomarker for excitatory responses in the brain and hence attenuated the level of tau protein and its phosphorylated form. These results indicated that a novel therapeutic strategy was involved in AD management. Riluzole is under clinical investigation for cognitive enhancement in Phase II trial with donepezil adjunct therapy in mild to moderate AD patients (C.T.I.: NCT01703117) [Mokhtari et al. 2017]. Verubecestat (MK-8931) is an inhibitor of BACE1 and plays an appropriate part in minimizing the A $\beta$  production in several animal models and in AD patients (Figure 2.21). In 2017, due to lack of efficacy and inappropriate findings, they discontinued the clinical trial studies in mild-to-moderate AD patients (C.T.I.: NCT01739348) [Ghezzi et al. 2013]. Another orally available EVP-0962 is considered as a selective  $\gamma$ -secretase modulator that plays an appropriate character in reducing the formation of A $\beta$ <sub>(1-42)</sub>. However, the result revealed that EVP-0962 produced promising effects in transgenic Alzheimer's models, attenuating A $\beta$ <sub>(1-42)</sub> level, reversing cognitive dysfunction, with improved behavioral deficits, and with diminished inflammation related to AD. EVP-0962 was attenuated in Phase II clinical investigations in the USA (C.T.I.: NCT01661673) (Figure 2.21) [Piton et al. 2018]. Ispronicline (AZD-3480) is a selective agonist of the nicotinic receptor  $\alpha$ 4 $\beta$ 2 and was regarded as a candidate which can improve cognitive dysfunction as well as memory enhancement but the results in phase 2 revealed that ispronicline (Figure 2.22) could not produce a significant effect in mild to moderate AD patients (NCT01466088) [Haydar and Dunlop 2010].

Epigallocatechin-3-gallate (EGCg) (Figure 2.22), a polyphenol from green tea, plays a significant part in the induction of  $\alpha$ -secretase as well as in preventing the A $\beta$  aggregation in animals by directly interacting with the cavity of the misfolded or unfolded peptides. EGCg also modulates several cellular mechanistic pathways, i.e. signal transduction pathways and mitochondrial function. EGCg has now undergone in phase 2–3 RCT in patients with early AD (NCT00951834) [Mecocci and Polidori 2012].

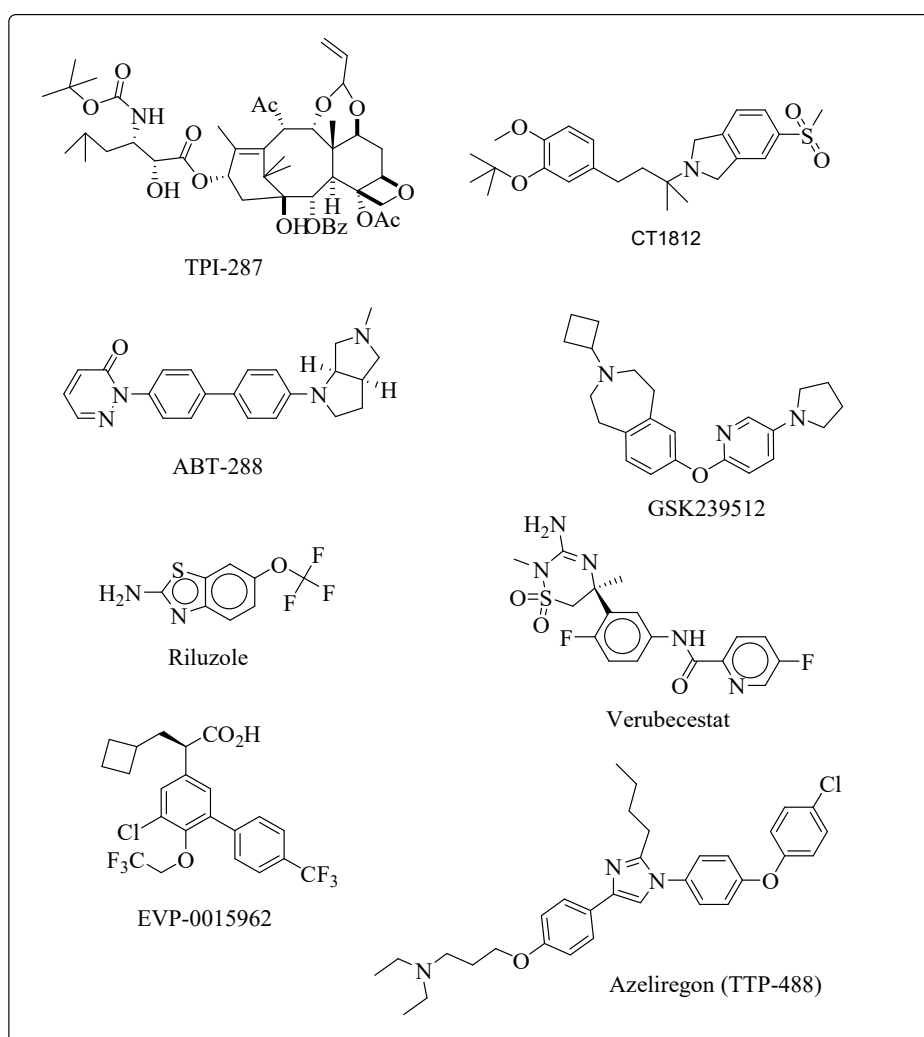


**Figure 2.21.** Structures of the compounds under clinical investigations

Several GSK3 inhibitors are under optimization for AD therapy and amongst them, NP-031112 (Figure 2.22) is a thiadiazolidinone derivative regarded as a non-ATP antagonist of GSK3 and has shown the reduction of phosphorylated tau and amyloid deposition level

in the brain and ultimately prevented neuronal death in animals. This drug has been analyzed in mild-moderate AD patients in a phase 2 RCT (NCT00948259) but no relevant clinical findings have yet been published [Liu et al. 2014].

### **2.3.3. Phase III**

Azeliragon (TTP-488) (Figure 2.21) is a small molecule and a specific competitive inhibitor of receptors for advanced glycation end products (RAGE). It is hypothesized that when advanced glycation end products (AGE) bind with the RAGE, it potentiates the formation of inflammatory responses and initiates oxidative processes. Ultimately, binding of this RAGE with A $\beta$  leads to the production of toxic A $\beta$  aggregation and hence initiates the AD pathology. A phase 3 study on the RAGE inhibitor TTP488 is ongoing (NCT02080364) [Cherian and Gohil 2015]. Another orally administered drug i.e. Tramiprosate (Figure 2.22) selectively binds with the A $\beta$  and makes it in soluble form but the result of phase 3 trial data suggested that it could not produce any effective clinical findings in mild to moderate AD patients (C.T.I.: NCT00314912) [Aisen et al. 2011]. Idalopirdine (Lu AE58054) is a 5-HT<sub>6</sub> serotonin inhibitor that has shown significant efficacy and safety data in Phase II investigation and also played a significant role in cognitive dysfunction and memory enhancement linked with AD. However, idalopirdine is safe and works with donepezil as an adjunct therapy in patients with mild-to-moderate AD. Idalopirdine did not achieve its efficacy endpoint versus placebo in the current two-phase III investigations (C.T.I.: NCT02006641) [Bennett 2018]. Encenicline (EVP-6124, MT-4666), a partial selective agonist of  $\alpha$ 7nAChR, has been developed to cure and manage cognitive deformities and memory improvement in AD patients. Based on the clinical findings, it was assumed that encenicline (Figure 2.22) could be considered as a useful agonist of nicotinic receptor to uplift cognitive effects. In 2015, two Phase III

clinical investigations U.S. FDA has halted the further trials on encenicline due to gastrointestinal problems (C.T.I.: NCT01969136 and NCT01969123) [Keefe et al. 2015]. Bapineuzumab, humanized monoclonal antibody that interact with the N-terminal epitope A $\beta$  in the brain and potentiate the therapeutic effect in AD. The clinical finding stated that it was ended in two Phase III clinical investigations due to lack of efficacy in mild-to-moderate AD patients (C. T.I.: NCT00667810 and NCT00676143) [Salloway et al. 2014]. Crenezumab was potentially identified as oligomeric A $\beta$  peptides with a higher affinity and specificity for amyloid plaques. Crenezumab clinical investigation had started registering mild AD patients for Phase III study in 2016, which has run until 2020 (C.T.I.: NCT02670083) [Cummings et al. 2018]. Aducanumab has the potency to bind with amyloid plaques and leads to its disaggregation and significantly attenuated the level of A $\beta$  plaques. Aducanumab has recently been approved by the FDA through accelerated approval pathway in a controversial manner due to ambiguous clinical trial data produced by Biogen related to its efficacy [O'Gorman et al. 2017]. TRx0237 (LMTM) (Figure 2.22) is considered as a second-generation hyper-activation tau inhibitor and it is under Phase III clinical investigations. Findings of the first Phase III trial in mild AD condition are still awaited (C.T.I.: NCT01689233). The second Phase III trial in mild-to-moderate AD conditions produced unfavorable outcomes (C.T.I.: NCT01689246) [Qian et al. 2015]. Flurizan<sup>TM</sup> (r-flurbiprofen) (Figure 2.22) is a non-steroidal anti-inflammatory drug (NSAID) that is analogous and homologous to ibuprofen which can be utilized to treat inflammatory responses in the AD brain. But based on the clinical studies, Flurizan<sup>TM</sup> was discontinued in a Phase III trial because of inappropriate findings in mild AD patients (C.T.I.: NCT00322036) [Wilcock et al. 2005]. Epidemiological studies demonstrated that hypertension leads to cognitive alteration and nilvadipine (Figure 2.22) is considered as a calcium channel inhibitor in the management of AD. The clinical studies revealed that

nilvadipine significantly reduces A $\beta$  plaque formation in the brain. Now, the Phase III clinical investigation of nilvadipine has been finished in mild-to-moderate AD patients and results are awaited (C.T.I.: NCT02017340) [Lawlor et al. 2018].

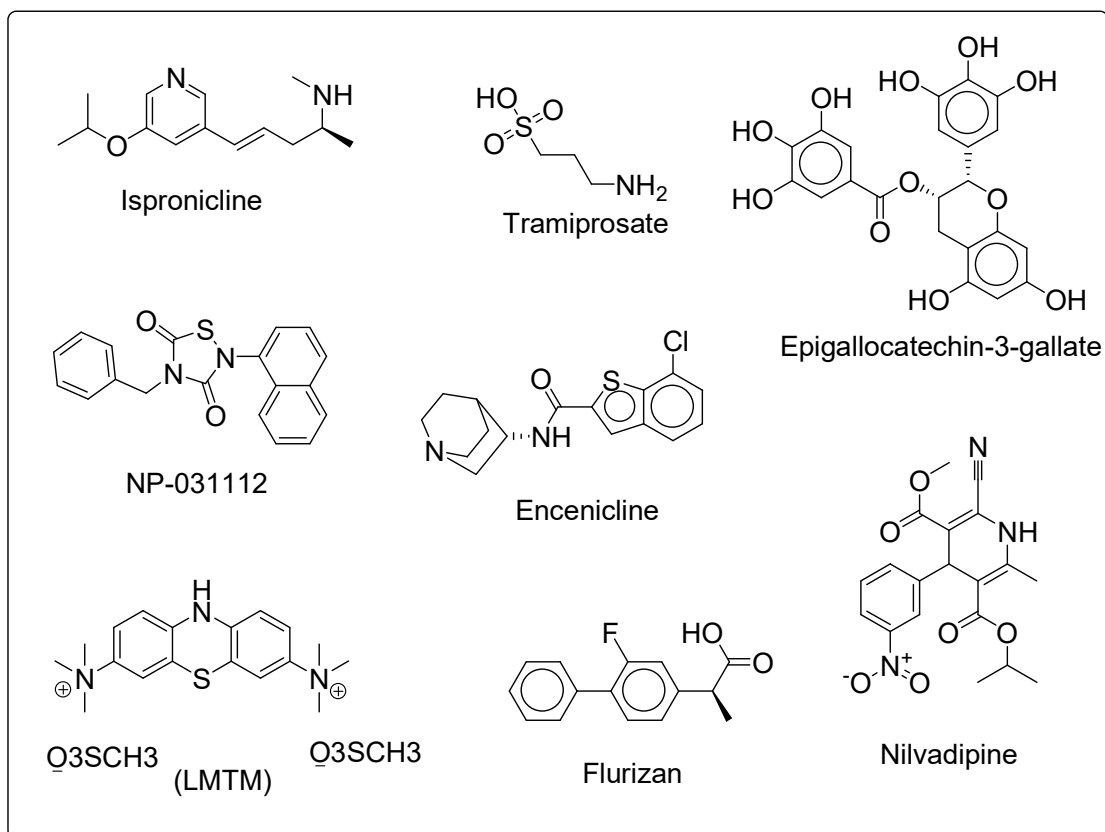


**Figure 2.22.** Structures of the compounds under clinical phase

**Table 2.1.** Drugs and vaccines under clinical trials for AD therapy.

S.No .	Name of compound	Clinical trial phase and status	Activity profile	C.T.I. No.
1.	AD-01, AD-02	Phase I	A $\beta$ inhibition	NCT01225809, NCT02008513
2.	TPI 287	Phase I	Microtubule Stabilizing Agent	NCT01966666
3.	CT1812	Phase I	Sigma-2 receptor antagonist	NCT03522129
4.	UB-311	Phase II	Anti-A $\beta$ immune activity	NCT03531710

6.	ABT-288	Phase II	H <sub>3</sub> receptor inhibitor	NCT01018875
7.	GSK239512	Phase II	H <sub>3</sub> receptor inhibitor	NCT01009255
8.	Riluzole	Phase II	Tau phosphorylation inhibition	NCT01703117
9.	Verubecestat	Phase II	BACE-1 inhibitor	NCT01739348
10.	EVP-0962	Phase II	$\gamma$ -secretase inhibitor	NCT01661673
11.	Ispronidine	Phase II	Nicotinic Receptor Agonist	NCT01466088
12.	Epigallocatechin-3-gallate	Phase II	$\alpha$ -secretase	NCT00951834
13.	NP-031112	Phase II	Non-ATP GSK3 antagonist	NCT00948259
14.	Azeliragon	Phase III	RAGE inhibitor	NCT02080364
15.	Tramiprosate	Phase III	A $\beta$ inhibition	NCT00314912
16.	Idalopirdine	Phase III	5-HT <sub>6</sub> serotonin antagonist	NCT02006641
17.	Bapineuzumab	Phase III	A $\beta$ aggregation inhibition	NCT00667810 NCT00676143
18.	Crenezumab	Phase III	A $\beta$ aggregation inhibition	NCT02670083
19.	Aducanumab	FDA approved	A $\beta$ disaggregation	-
20.	TRx0237	Phase III	Tau-protein inhibition	NCT01689233 NCT01689246
21.	Flurizan	Phase III	NSAIDS	NCT00322036
22.	Nilvadipine	Phase III	Calcium channel blocker and inhibit A $\beta$ aggregation	NCT02017340

#### 2.4. Available neuro-therapeutics for AD treatment

Reversible AChE blockers play a significant role in enzymatic activity alterations. Four FDA-approved drugs including three AChE inhibitors namely donepezil, rivastigmine,

galantamine, and one NMDA inhibitor which is memantine currently used to treat AD symptomatically. Donepezil (Figure 2.23) is an N-benzyl piperidine analog that is a non-competitive, reversible, AChE inhibitor that helped in the management of cognitive impairments and memory enhancement by maintaining the level of extracellular ACh. It also showed attenuated neuronal toxicity in a dose-dependent regime [Birks and Harvey 2018]. Rivastigmine (Figure 2.23) is another widely used reversible ChE inhibitor molecule. Its carbamate scaffold provides higher selectivity towards AChE over BuChE and makes it a good candidate possessing a significant pharmacological profile. It is prominently used in mild to moderate AD patients [Weinstock 1999]. Similarly, galantamine (Figure 2.23) acts as a dual inhibitor of AChE in conjugation with allosteric alteration to nicotinic acetylcholine receptors (nAChR) and ultimately enhances the ACh level. However, it showed some gastrointestinal side effects and was less tolerated as compared to other AD drugs [Olin and Schneider 2002]. Additionally, memantine (Figure 2.23) is an uncompetitive glutamatergic NMDA receptor antagonist and modulates the  $\text{Ca}^{2+}$  influx and provides symptomatic treatment in the management of AD [Molinuevo et al. 2005]. Recently, Aducanumab and Lecanemab (monoclonal antibodies) have been approved by FDA in an accelerated approval pathway as a disease-modifying therapy for AD. Aducanumab and Lecanemab both are associated with improvements in memory and cognitive impairments linked to  $\text{A}\beta$  plaques, though their use is still controversial in AD progression.

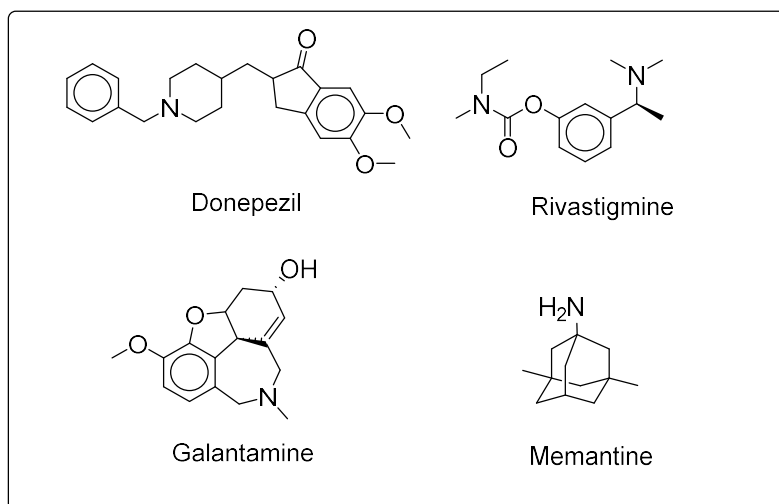


**Figure 2.23.** FDA approved drugs for AD treatment

